HHS Public Access

Author manuscript

Environ Sci Technol. Author manuscript; available in PMC 2022 September 21.

Published in final edited form as:

Environ Sci Technol. 2021 September 21; 55(18): 12291–12301. doi:10.1021/acs.est.1c01200.

Rapid Characterization of Human Serum Albumin Binding for Per- and Polyfluoroalkyl Substances Using Differential Scanning Fluorimetry

Thomas W. Jackson, **Chris M. Scheibly**, **M. E. Polera**, **Scott M. Belcher**

Center for Human Health and The Environment Department of Biological Sciences, North Carolina State University, Raleigh, North Carolina 27695, United States

Abstract

Per- and polyfluoroalkyl substances (PFAS) are a diverse class of synthetic chemicals that accumulate in the environment. Many proteins, including the primary human serum transport protein albumin (HSA), bind PFAS. The predictive power of physiologically based pharmacokinetic modeling approaches is currently limited by a lack of experimental data defining albumin-binding properties for most PFAS. A novel thermal denaturation assay was optimized to evaluate changes in the thermal stability of HSA in the presence of increasing concentrations of known ligands and a structurally diverse set of PFAS. Assay performance was initially evaluated for fatty acids and HSA-binding drugs ibuprofen and warfarin. Concentration–response relationships were determined and dissociation constants (K_d) for each compound were calculated using regression analysis of the dose-dependent changes in HSA melting temperature. Estimated K_d values for HSA binding of octanoic acid, decanoic acid, hexadecenoic acid, ibuprofen, and warfarin agreed with established values. The binding affinities for 24 PFAS that included perfluoroalkyl carboxylic acids (C4–C12), perfluoroalkyl sulfonic acids (C4–C8), mono- and polyether perfluoroalkyl ether acids, and polyfluoroalkyl fluorotelomer substances were determined. These results demonstrate the utility of this differential scanning fluorimetry assay as a rapid high-throughput approach for determining the relative protein-binding properties and identification of chemical structures involved in binding for large numbers of structurally diverse PFAS.

Graphical Abstract

Corresponding Author: Scott M. Belcher – Center for Human Health and The Environment Department of Biological Sciences, North Carolina State University, Raleigh, North Carolina 27695, United States; Phone: 919-513-1214; smbelch2@ncsu.edu.

Complete contact information is available at: https://pubs.acs.org/10.1021/acs.est.1c01200

The authors declare no competing financial interest.

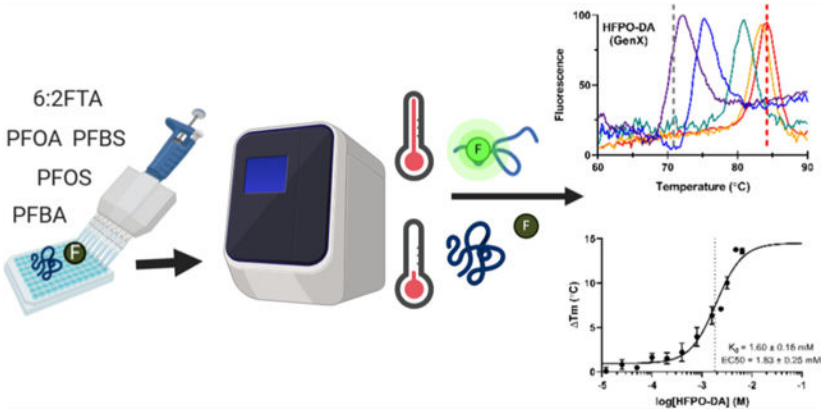

Keywords

alcohols; carboxylic acids; fluorocarbons; perfluorocarbons; protein; sulfonic acids; telomer; thermal stability; toxicokinetic

1. INTRODUCTION

Per- and polyfluoroalkyl substances (PFAS) are a large class of persistent synthetic chemicals used in a wide variety of industrial and consumer applications.[1–3] The perfluorinated aliphatic backbones of PFAS are hydrophobic, chemically inert, and thermally stable; consequently, they are persistent and accumulate in the environment and in biota.[4] The most recent comprehensive analysis by the Organization of Economic Cooperation and Development identified >4730 PFAS-related CAS registry numbers, including 947 compounds that were registered in the EPA Toxic Substances Control Act (TSCA) chemical inventory.[5]

Production and use of long-chain perfluoroalkyl acids (PFAA) (e.g., perfluoroalkylcarboxylic acids (PFCA) with ≥7 fluorinated carbons and perfluoroalkylsulfonic acids (PFSA) with ≥6 fluorinated carbons) began in the 1950s and continued in the U.S. until 2002, when manufacturers began to phase out long-chain PFAA due to their persistence and toxicity. As a response to the phase out, short-chain PFAS are increasingly used as replacements in many applications and processes.[6] Common examples include PFCA and PFSA with shorter fluoroalkyl chains [e.g., perfluorobutanecarboxylic acid (PFBA) and perfluorobutanesulfonic acid (PFBS)], per- and polyfluoroalkyl ether acids (PFEA) that contain one or more ether moieties [e.g., hexafluoropropylene oxide dimer acid (HFPO-DA)], and fluorotelomer acids and alcohols with perfluoroalkyl length ≤6.[1,7,8] Since their introduction, shorter-chain replacement PFAS are now detected ubiquitously in the environment and are accumulating in people and other organisms across the world.[9–11]

The physiochemical properties, exposure, and toxicity of perfluorooctanoic acid (PFOA) and perfluorooctanesulfonic acid (PFOS) are most well characterized. By contrast, there are only limited data available for the majority of known PFAS, including most of the replacement PFAS currently in use. The thousands of PFAS for which there is a paucity

of available data necessitate the use of high-throughput and predictive computational strategies to characterize the physiochemical properties, bioactivity, and potential toxicity across different classes of PFAS. Recently, physiologically based pharmacokinetic and molecular dynamics modeling, quantitative structure–activity relationship, and machine learning approaches have been developed to predict protein-binding affinity for PFAS.[12,13] The predictive capabilities of these approaches are currently limited by a lack of data defining fundamental physiochemical and toxicokinetic properties for most PFAS.

Albumin, the primary transport protein for PFOS, PFOA, perfluorononanoic acid (PFNA), perfluorohexanesulfonic acid (PFHxS), and perfluorodecanoic acid (PFDA), contains multiple nonspecific binding sites that selectively bind fatty acids, hormones, drugs, and some xenobiotics including PFAS.[14] However, experimentally determined binding affinities of most PFAS at albumin are unavailable. Current approaches for determining protein-binding affinities, including titration chemistry or surface plasmon resonance, are too resource intensive and time-consuming to individually determine albumin affinity for each of the thousands of different PFAS.

Differential scanning fluorimetry (DSF) is a rapid high-throughput method for measuring ligand binding interactions that is most often used to assess protein stability under various conditions.[15–17] The DSF assay employs an environmentally sensitive fluorophore that is quenched while free in solution. Binding of the dye to hydrophobic sites accessible as the protein unfolds as temperature rises causes unquenching and fluorescence proportional to the amount of bound dye.[18,19] Protein binding of ligand causes a concentration- and affinity-dependent stabilization of the folded protein structure observed as an increase in the melting temperature (T_m).[16,20,21] Relative binding affinity of the stabilizing ligand can be calculated from the dose–response relationship for the change in the T_m.[17]

The goal of this study was to develop and optimize a high-throughput DSF assay to rapidly characterize the relative human serum transport protein albumin (HSA) binding affinity of a variety of different PFAS. An initial set of control compounds, including fatty acids and albumin-binding drugs ibuprofen and warfarin, which bind HSA at different binding sites, were used to demonstrate feasibility and evaluate whether binding affinities estimated from DSF were comparable to known values estimated by other methods. Following optimization of DSF for PFOA and PFOS, the binding affinity at HSA was determined for a structurally diverse set of PFAS that included nine perfluoroalkyl carboxylic acids of increasing chain length (C4–C12), three perfluoroalkyl sulfonic acids, four ether-containing PFAS, and eight fluorotelomer substances. The results from these analyses reveal that DSF approaches can be used to define protein-binding affinities rapidly and accurately for large numbers of chemically distinct PFAS, and this approach is able to discriminate between structurally similar PFAS. These results provide essential experimental data to better understand this diverse group of environmental contaminants.

2. MATERIALS AND METHODS

2.1. Chemicals and Reagents.

Reagents and solvents used were of the highest purity available. All aqueous buffers and solutions were prepared in sterile Milli-Q A10 water (18 Ω; 3 ppb total oxidizable organics). GloMelt (λ_{Ex} = 468, λ_{Em} = 507 nm) and carboxyrhodamine (ROX; λ_{Ex} = 588, λ_{Em} = 608 nm) dyes were purchased from Biotium (Fremont, CA). The PFAS analyzed are shown in Figure 1. Octanoic acid (CAS 124-07-2, purity ≥ 98%), perfluorobutanoic acid (PFBA, CAS 375-22-4, purity ≥ 99%), perfluoropentanoic acid (PFPeA, CAS 2706-90-3, purity ≥ 97%), perfluoroheptanoic acid (PFHpA) (CAS 375-85-9, purity ≥ 98%), PFOA (CAS 335-67-1, purity ≥ 95%), perfluorodecanoic acid (PFDA, CAS 335-76-2, purity ≥ 97%), perfluorododecanoic acid (PFDoA, CAS 307-55-1, purity ≥ 96%), perfluorotetradecanoic acid (PFTDA, CAS 376-06-7, purity ≥ 96%), and HFPO-DA (CAS 13252-13-6, purity ≥ 97%) were from Alfa Aesar (Havermill, MA). Perfluorohexanoic acid (PFHxA, CAS 307-24-4, purity ≥ 98%), perfluorononanoic acid (PFNA, CAS 375-95-1, purity ≥ 95%), perfluorobutanesulfonic acid (PFBS, CAS 375-73-5, purity ≥ 98%), warfarin (CAS 81-81-2, purity ≥ 98%), and 1*H*,1*H*,2*H*,2*H*-perfluorohexane-1-ol (4:2 FTOH, CAS 2043-47-2, purity ≥ 97%) were from TCI America (Portland, OR). Perfluoroundecanoic acid (PFunDA, CAS 2058-94-8, purity ≥ 96%) was from Oakwood Chemical (Estill, SC), perfluorohexanesulfonic acid (PFHxS, CAS 3871-99-6, purity ≥ 98%) was from J&K Scientific (Beijing, China), and PFOS (CAS 2795-39-3, purity ≥ 98%) and perfluoro-3,6,9-trioxadecanoic acid (PFO3DoDA, CAS 151772-59-7, purity 98%) were from Matrix Scientific (Columbia, SC). Nafion byproduct 2 (CAS 749836-20-2, purity ≥ 95%), 1,1,1,2,2,3,3-heptafluoro-3-(1,2,2,2-tetrafluoroethoxy)propane (E1, CAS 3331-15-2, purity ≥ 97%), 1*H*,1*H*,2*H*,2*H*-perfluorooctanol (6:2 FTOH, CAS 647-42-7, purity ≥ 97%), 2*H*,2*H*,3*H*,3*H*-perfluorohexanoic acid (3:3 FTCA, CAS 356-02-5, purity ≥ 97%), 2*H*,2*H*,3*H*,3*H*-perfluorooctanoic acid (5:3 FTCA, CAS 914637-49-3, purity ≥ 97%), 2,*H*,2*H*,3*H*,3*H*-perfluorononanoic acid (6:3 FTCA, CAS 27854-30-4, purity ≥ 97%), 2,*H*,2*H*,3*H*,3*H*-perfluoroundecanoate (8:3 FTCA, CAS 83310-58-1, purity ≥ 97%), 2*H*,2*H*,3*H*,3*H*-perfluorohexanesulfonic acid (4:2 FTSA, CAS 757124-72-4, purity ≥ 97%), and 2*H*,2*H*,3*H*,3*H*-perfluorooctane-1-sulfonate (6:2 FTSA, CAS 59587-39-2, purity ≥ 97%) were from Synquest Laboratories (Alachua, FL). HSA (CAS 70024-90-7, purity ≥ 95%, fraction V fatty acid free) and hexadecanoic acid (CAS 57-10-3, natural, purity ≥ 98%) were from MilliporeSigma (Burlington, MA). HEPES (4-(2-hydroxyethyl)-1-piperazineethanesulfonic acid), sodium chloride, methanol, dimethyl sulfoxide, decanoic acid (CAS 334-48-5, purity ≥ 99%), ibuprofen (CAS 15687-27-1, purity ≥ 99%), and potassium chloride (KCl, CAS 7447-40-7, purity ≥ 99.7%) were purchased from Thermo Fisher (Waltham, MA).

2.2. Control and Test Chemical Preparation.

Stock solutions (20 mM) of PFBA, PFPeA, PFHxA, PFHpA, PFOA, PFBS, PFHxS, PFOS, HFPO-DA, Nafion bp2, 6:3 FTCA, 6:2 FTSA, decanoic acid, ibuprofen, and KCl were prepared in aqueous 1× HEPES-buffered saline (HBS, 140 mM NaCl, 50 mM HEPES, 0.38 mM Na_2HPO_4, pH 7.2). A 1:1 mixture of HBS and dimethyl sulfoxide (DMSO) was used as a solvent for PFNA, PFDA, PFunDA, and 8:3 FTCA stocks due to limited

aqueous solubility, and the fatty acids and warfarin were dissolved in HBS supplemented with 30% methanol. For experiments evaluating possible solvent effects, 20 mM stock solutions of PFOA were prepared in all three solvents. The HBS concentrations used in solvents containing DMSO or methanol were adjusted to ensure that the final concentration of the thermal denaturation buffer contained 140 mM NaCl, 50 mM HEPES, and 0.38 mM Na_2HPO_4. Solution pH for PFAS stocks was confirmed to be 7.4 and stocks were stored at −20 °C. For thermal stability concentration–response analysis, stock solutions were serially diluted into solvents. Stocks of HSA (1 mM) were prepared in 2× HBS and then diluted with an equal volume of H_2O to final desired concentrations.

2.3. Differential Scanning Fluorimetry.

Temperature control and fluorescence detection were performed using a Step One Plus Real-Time PCR System (Applied Biosystems; Grand Island, NY) with indicator dye (GloMelt) fluorescence (λ_{Ex} = 468 λ_{Em} = 507 nm) detected using the FAM/SYBR filter set and the passive reference dye carboxyrhodamine (λ_{Ex} = 588 λ_{Em} = 608 nm) detected using the ROX channel. Thermal denaturation was performed in sealed optical 96 well reaction plates (MicroAmp Fast, Applied Biosystems) using the following conditions: 10 min at 37 °C for one holding stage, followed by a ramp profile from 37 to 99 °C at a rate of 0.2 °C/s. Following optimization, each DSF assay contained 0.125 mM HSA in a final volume of 20 μl. Stock solutions of each test chemical were serially diluted into HBS, with final concentrations ranging from 50 μM to 10 mM. Working fluorophore solutions (200× in 0.1% DMSO) diluted 1:20 and ROX (40 μM) diluted 1:10 were prepared immediately prior to each experiment with 2 μl of each used for each assay. At least two independent plates were run for each experimental unit. Controls run on each plate included matching vehicle control (no ligand; KCl added for potassium salts), no protein control, and a minimum of three concentrations of decanoic acid as a positive control for protein stabilization. To evaluate the sensitivity of the assay to detect DMSO-mediated conversion of hexafluoropropylene oxide dimer acid (HPFO-DA) to E1,[22] HFPO-DA was prepared in a 1:1 mixture of HBS and DMSO and maintained at room temperature for 4 h before experimental analysis. To evaluate whether volatile compounds were entering the gas phase to reduce concentrations of PFAS, experiments were performed using different reaction volumes ranging from 10 to 200 μL in each well for 4:2 FTOH, 6:2 FTOH, PFHxS, and 6:2-FTS.

2.4. Data Analysis and Statistics.

All presented DSF data are representative of multiple experiments each containing three replicates for each sample. Matching vehicle blank controls lacking the test compound were included on the same plate for each experiment. Raw thermocycler data were exported to Excel (Microsoft) and statistical analysis was performed using SPSS v26 (IBM, Armonk, NY) or GraphPad Prism (v8.3.0, GraphPad Software Inc., San Diego, CA). Data are reported as mean values ± SD following background subtraction. Assay data is reported in relative fluorescent light units (RFU). T_m is defined as the temperature at which the maximum change in fluorescence is observed, indicating half of the protein is unfolded. PFAS concentration–response curves were smoothed using the Savitzky and Golay method,[23] EC_{50} estimates are derived using a 4-parameter variable slope model,

and dissociation constants were calculated by a single-site ligand binding model using the formula[24]

$$Y = \text{bottom} + (\text{top} - \text{bottom}) \times \left[1 - \frac{P - K_d - X + \sqrt{(P + X + K_d)^2 - 4PX}}{2P}\right]$$

in which top is the maximal response, bottom is the minimal response, P is the protein concentration, K_d is the dissociation constant, X is the ligand concentration, and Y the is change in T_m. This equation requires that a maximal response be detected, which is limited by the solubility of the compounds of interest. This equation fits a concentration–response curve to the melt shift and provides an estimated dissociation constant. Using this equation, the calculated K_d is most accurate when its value is greater than 50% of the protein concentration and requires ligand concentrations ~10 times the K_d.[24]

The relationship between the number of aliphatic carbons or number of fluorine and the binding affinity of HSA for each compound was determined using a second-order polynomial (quadratic) best fit with least-squares regression. Comparison between protein concentrations and comparisons of calculated binding affinities between different compounds was performed using one-way analysis of variance (ANOVA) and a Tukey's post hoc test was performed to evaluate pairwise differences. Significance between differences in values was defined as $p < 0.05$.

3. RESULTS

3.1. Thermal Melt Assay Optimization.

Concentrations of HSA between 0.05 and 0.625 mM were evaluated to identify the HSA concentration that yielded maximal signal-to-noise ratio (Figure 2A). The observed T_m for HSA (71.3 °C) did not vary across the concentration range analyzed ($F(4, 10) = 2.19$, $p = 0.14$; Figure 2B). Optimal performance was observed in assays containing 0.125 mM HSA (Figure 2A). Including an initial 10 min preincubation at 37 °C decreased the relatively high initial fluorescence observed for HSA, and the optimal temperature ramp rate was determined to be 0.2 °C/s.

Most study compounds were sufficiently soluble to use 1x HBS as a solvent for 20 mM stock solutions. The limited aqueous solubility of the C9-C11 PFCA and 8:3 FTCA required use of HBS containing 50% DMSO, and the fatty acids and warfarin required using 30% methanol as a solvent. Possible solvent effects were investigated for PFOA that was solubilized in each of the three solvents. Assay results for HSA binding of PFOA were not significantly influenced by the stock solution solvent ($F(2, 15) = 0.005$, $p = 0.996$) (Table 1). The increase in potassium ions from the potassium salts of PFHxS, PFOS, 8:3 FTCA, and 6:2 FTSA did not affect the assay results (data not shown).

3.2. Measurement of HSA-Binding Affinity for Known HSA-Binding Compounds.

Octanoic acid, decanoic acid, hexadecenoic acid, warfarin, and ibuprofen were used as positive controls to evaluate whether DSF estimates of binding affinities were comparable

to published values using other methods. Analysis of the fatty acid-induced melting temperature shift of HSA determined a K_d of 2.10 ± 0.47 mM for octanoic acid, 0.74 ± 0.32 mM for decanoic acid (Figure 2C,D), and 0.030 ± 0.02 mM for hexadecanoic acid (Table 2). Two-way ANOVA revealed that the fatty acids were significantly different (F(2, 15) = 63, $p < 0.0001$), with Tukey's post hoc comparison indicating that each fatty acid was significantly different from the other two examined. The calculated K_d for HSA binding of ibuprofen was 2.39 ± 0.88 mM (Figure 2E,F) and of warfarin was 0.16 ± 0.10 mM (Table 2). The calculated affinities of HSA binding for each of all compounds are within the range of previously determined values.[32–35]

3.3. Measurement of HSA-Binding Affinity for PFAS.

Numerous studies have evaluated albumin binding of PFOA and PFOS.[26–31] Using DSF, the calculated K_d for HSA binding of PFOA was 0.83 ± 0.38 (Figure 3A,B) and of PFOS was 0.69 ± 0.078 mM (Figure 3C,D and Table 3). The calculated K_d values for HSA binding of PFOA and PFOS were similar to previously reported values, although these values vary greatly depending on the method and assay conditions.[26–31] The findings from the DSF assay and calculated dissociation constant for each PFCA (C4–C12), PFSA (C4–C8), ether-containing PFAS (PFAE; Figure 3E,F), and eight fluorotelomer compounds are shown in Table 3. It is notable that the fluorotelomer alcohols 4:2 FTOH and 6:2 FTOH were not bound by HSA and that fluorotelomer compounds with a carboxylate or sulfonate charged group were bound by HSA at affinities similar to those observed for PFAA with the same number of aliphatic carbons (Table 3).

To determine whether the high volatility of the fluorotelomer alcohols was responsible for the absence of albumin binding, values were determined for 4:2 FTOH, 6:2 FTOH, PFHxS, and 6:2-FTS at volumes of 10, 20, 50, and 200 μL that resulted in different volumes of the gaseous phase in each sealed reaction well. At 200 μL, the well has no gas phase. There were no differences in the thermal shift profile at different volumes for any of the four PFAS measured, findings that suggest that the volatility of the fluorotelomer alcohols was not responsible for the lack of albumin binding (4:2 FTOH, F(3, 8) = 0.90, $p = 0.48$; 6:2 FTOH, F(3, 8) = 0.14, $p = 0.93$; PFHxS, F(3, 8) = 0.63, $p = 0.61$; 6:2 FTSA, F(3, 8) = 0.67, $p = 0.60$).

To investigate the sensitivity of the assay to distinguish binding properties for closely related compounds, we compared assay results for HFPO-DA prepared in aqueous buffer or in DMSO-containing buffer with assay results for E1 directly. In DMSO, HFPO-DA is rapidly converted to E1 via decarboxylation.[22] Two-way ANOVA of the area under the curve of the concentration–response curves for HFPO-DA in DMSO, HFPO-DA in buffer alone (Figure 3G), and E1 reveals significant differences (F(2, 29) = 144, $p < 0.0001$), with Tukey's post hoc analysis indicating that HFPO-DA in DMSO is indistinguishable from the E1 curve with EC_{50} values of 2.34 ± 0.56 and 2.36 ± 0.42 mM, respectively ($p = 0.98$; Figure 3H). Tukey's post hoc analysis found that HFPO-DA in buffer alone is significantly different from HFPO-DA in DMSO and E1 in buffer (both $p < 0.0001$).

3.4. Physiochemical Determinants of HSA Binding.

To interrogate the determinants of HSA binding of PFAS in more detail, the relationship between calculated binding affinities and the number of per- and polyfluorinated carbons, the number of aliphatic carbons or total fluorine numbers for the PFCA series from C4 to C12 and across all compounds were analyzed. Except for the PFAE compounds, highest affinity was observed for compounds containing 6–8 fluorinated carbons, 7–9 aliphatic carbons, and containing 13–17 fluorine (Figure 4). For the PFAE, a simple linear regression was more appropriate. For the PFCA series from C4 to C12, the best-fit curve for the relationship between binding affinity and the number of per- and polyfluorinated carbons was $Y = 6.30 - 1.50X + 0.10X^2$ (Figure 4A; $R^2 = 0.88$) and for all compounds except PFAEs was $Y = 4.73 - 1.08X + 0.074X^2$ ($R^2 = 0.54$). For PFAE, this relationship was best described by the simple linear regression equation $Y = -0.02X + 1.7$ (Figure 4B; $R^2 = 0.79$). Except for the PFAE, the best-fit curve for the realtionship between number of aliphatic carbons and binding affinity was $Y = 6.52 - 1.39X + 0.083X^2$ (Figure 4C; $R^2 = 0.69$) and Y = for the number of fluorine (Figure 4D; $R^2 = 0.54$). For the PFAE family, the relationship between affinity and number of aliphatic carbons was $Y = -0.06X + 1.9$ (Figure 4C; $R^2 = 0.52$) and $Y = -0.01X + 1.7$ for number of fluorines (Figure 4D; $R^2 = 0.77$).

4. DISCUSSION

4.1. Optimization and Demonstration of Assay Utility.

The goal of the current studies was to develop a rapid, high-throughput assay capable of measuring protein-binding affinity of a diverse collection of PFAS compounds. The presented experiments describe the optimization and use of a DSF assay for assessing HSA-binding properties for control compounds known to bind albumin and 24 PFAS from six subclasses. Critical initial experiments aimed to optimize DSF for measuring PFAS binding included determination of optimal protein and dye concentrations to maximize the signal-to-noise ratio. Those efforts were found especially critical for determining albumin binding due to its multiple surface-accessible hydrophobic binding sites that increased baseline fluorescence.[32] Additional key factors analyzed during assay development included use of a HEPES buffer to ensure that PFAS with low pK_a did not affect the assay pH, maintaining consistent ionic strength, determination of appropriate solvents, and optimization of assay temperature ramp rates. Results of these initial experiments identified appropriate conditions for determining the binding affinities of structurally diverse sets of natural fatty acids, small molecule pharmaceuticals, and multiple subclasses of PFAS in a rapid (<3 h) format. The accuracy and reproducibility of the binding affinities calculated using DSF were demonstrated for known albumin-binding drugs warfarin and ibuprofen, C10–C16 fatty acids, PFOA, and PFOS.[25–27,29,31,33–36] Further demonstrating the utility of this DSF thermal shift approach, comparative evaluation of the HSA-binding affinities of structurally diverse subclasses of PFAS revealed that functional groups, number of aliphatic carbons, and number of fluorine bonded to carbons were among the key physiochemical properties that influenced binding.

4.2. Impacts of Physiochemical Properties on HSA-Binding Affinity.

Published K_d values for HSA binding of fatty acids, drugs, and PFAS are variable and can span many orders of magnitude.[25–27,29,31,33,35–38] Because the absolute K_d values depend on the specific experimental conditions of each assay, it is most useful to compare relative affinities across different assays. The pattern of HSA affinity for fatty acids observed here is consistent with previous findings that found affinity increased with longer chain length such that the affinity of hexadecanoate > decanoate > octanoate.[33,37,38] For those fatty acids, increasing chain length allows the methylene tails to extend further into the deep hydrophobic cavities of HSA, with HSA-binding sites completely filled by fatty acids of length C18–C20.[39] While HSA can bind fatty acids longer than C20, binding affinity is decreased because the methylene tails are not fully accommodated and therefore have lower binding energies than optimal C16–C20 fatty acids.[39]

Some PFAS, specifically PFCA, have structural similarities with fatty acids, and the high-affinity fatty acid binding sites are likely sites for PFAS interactions.[40] Because PFCAs are analogous to fatty acids with fluorine replacing the aliphatic hydrogens, the same properties that allow albumin to bind fatty acids also allow albumin to bind PFAS. However, unlike fatty acids, PFAS have fluorinated alkyl tails that impart oleophobic amphiphilic surfactant properties and decrease the relative water solubility of PFAS.[41] Because of these complexities, numerous physiochemical properties, including the number of per- and polyfluorinated carbons, the number of aliphatic carbons, the number of fluorine attached to aliphatic carbons, and the functional headgroups, were evaluated for their influence on relative binding affinities of HSA for PFAS. Within each class of analyzed PFAS, the HSA relative affinity for aliphatic carbon length was C4–C5 < C6–C9 > C10+. The optimal structure for binding with HSA appears to be between six and nine aliphatic carbons. Unlike fatty acids, the increasing aliphatic backbone of C10 + PFAS appears to prevent optimal binding due to an increase in net negative charge resulting in oleophobic steric hindrances that may force the longer chain PFAA to fold.[40] Consistent with these observations, molecular docking experiments predict that PFAA with more than 11 carbons cannot easily fit into the binding pocket of fatty acid binding protein, but these molecular docking studies became less reliable for predicting HSA affinity for PFCA > 9 perfluorinated carbons due to a lack of experimental affinity data.[42] Ng and Hungerbuehler specifically emphasize the critical need for further experimental data on which to base molecular docking simulations, and the assay described here can provide this data via rapid comparison of protein affinity for multiple compounds assayed using the same experimental conditions.[42]

The importance of the functional headgroup in the affinity of HSA for PFAS was evaluated by comparing binding affinity between fluorotelomer compounds with an alcohol headgroup and those with a carboxylate or sulfonate headgroup. Strikingly, the two fluorotelomer alcohols tested, 4:2 FTOH and 6:2 FTOH, did not bind HSA. The fluorotelomer compounds with a carboxylate or sulfonate group were bound by HSA with affinities comparable to PFAA, demonstrating that the charged functional group is important for HSA binding. These findings are consistent with complexation energy analysis demonstrating the fluorinated chain of PFOA and PFOS interacted significantly with the aliphatic portion of the positively charged guanidinium groups of Arg 218 and Arg 222 and the backbone amine group of Asn

294, and these interactions were essential in the overall complexation between HSA and PFAS.[40] However, it is important to note that E1, an ether PFAS with no charged functional group, was also bound by albumin. It is likely that E1, and potentially other PFAE, is bound by albumin via a different mode than the other PFAS. This hypothesis is consistent with the binding patterns of fluorinated ether anesthetics, where there is evidence of nonpolar binding in subdomain IIIB by enflurane, a fluorinated ether anesthetic with a nominal dipole that contrasts with the polar binding by similar compounds with larger dipole moments (e.g., isoflurane).[43]

When comparing compounds with the same number of per- and polyfluorinated carbons but different functional groups, the binding affinity followed the pattern: ether acids < carboxylic acids < sulfonic acids. This pattern applied when comparing PFCA to PFSA and FTCA to fluorotelomer sulfonic acids. Previous reports demonstrate that the longer perfluorinated chain of PFOS provides greater complexation energy than PFOA, whereby apolar interactions account for much more of the binding between HSA and PFOS via increased van der Waals interactions.[40] That observation appears to hold true across classes, and increased van der Waals interactions provided by the additional fluorinated carbon in the PFSA of equal chain length to the PFCA explain the increased affinity of HSA for sulfonated moieties. Similarly, HSA had higher affinity for the fluorotelomer acids than the PFAA with equal numbers of per- and polyfluorinated carbons, providing further evidence that the number of aliphatic carbons provide increased stability with HSA by increasing the fit into the hydrophobic binding pockets. Finally, the findings that albumin had lower affinity for the PFEA than PFAA with the same number of per- and polyfluorinated carbons are consistent with previous work demonstrating that linear PFAS bind albumin much more strongly than their branched isomers, potentially reflecting that ether linkages impart structures similar to those adopted by branched isomers.[31]

4.3. Strengths and Limitations.

The DSF method utilized here has numerous advantages over typical methods including titration chemistry or surface plasmon resonance, namely, DSF requires substantially less protein (0.08 mg of HSA per assay) and the assay can be completed and provide affinity data for up to eight PFAS compounds in less than 4 h using the 96 well format. Ongoing studies have demonstrated that the assay is scalable to a 384 well format to further increase throughput. Additionally, DSF is performed using real-time PCR instruments that are widely available and accessible by most laboratories.[44] Further, this assay can be easily adapted to analyze binding affinities for a wide array of purified proteins and assay conditions.[16,45,46] It is important to note that DSF assays often employ the hydrophobic fluorophore SYPRO Orange; SYPRO Orange is not compatible with assays containing detergents or surfactants and is not useful for analyzing PFAS due to the amphipathic surfactant properties of many PFAS. The assay described here was optimized to use an alternative environment sensing fluorophore because of anticipated limitations of SYPRO Orange, namely, the surfactant and detergent-like properties of many PFAS would render the hydrophobic dyes incompatible.[24] Preliminary analysis found that a number of commercially available fluorescent rotor dyes, including (dicyanovinyl)julolidine, 9-(2-carboxy-2-cyanovinyl)julolidine, 4-(4-(dimethylamino)styryl)-*N*-methylpyridinium iodide,

and the used dye preparation GloMelt, were compatible for DSF analysis of PFAS (not shown).

An additional strength of this DSF assay is its ability to detect changes in PFAS chemistry, evidenced by the ability to detect the conversion of HFPO-DA to E1 following incubation in DMSO. Previous analysis has demonstrated that the use of DMSO as a solvent for HFPO-DA results in rapid and complete conversion of HFPO-DA to E1 in under 4 h.[22] Using this DSF assay, the complete decarboxylation of HFPO-DA by DMSO was demonstrated by the observed differences in the concentration–response relationship differences between HFPO-DA in HEPES-buffered saline and HFPO-DA in DMSO. The concentration–response curve and the resulting EC_{50} and HSA-binding affinity values for HFPO-DA in DMSO were found identical to that of E1 demonstrating the quantitative decarboxylation of HFPO-DA to E1.

However, we have demonstrated that PFAS compounds in aqueous solutions or prepared in the solvent methanol or DMSO were compatible with this assay, and the limited aqueous solubility of C12 and longer PFCA and other longer chain PFAS did not allow analysis across the concentration range needed to accurately determine binding affinities for HSA. Because the complete range of concentration–response must be determined to accurately evaluate the binding affinities and associated parameters, the DSF assay is limited to PFAS with sufficient solubility in aqueous solutions. Additionally, binding affinities determined using the DSF method are generated over a range of temperatures and are not directly related to dissociation constant values determined using other methods.[47] The ΔT_m used to calculate K_d has the advantage of giving a more complete view of the thermodynamic system when comparing compound binding. Consistent with previous reports that binding affinities calculated using DSF are often lower than using other methods due to calculating the affinity at melting temperature instead of physiological temperature, the absolute affinities of HSA for PFAS were lower but within the same order of magnitude of published values.[24] The differences in reported values are at least partly due to the fact that the dissociation constant is determined at the higher melting temperature of the protein with ligand, rather than at a constant temperature of 20 or 37 °C typically used for other methods.[34]

With these results, we have shown the utility of a rapid and sensitive high-throughput DSF assay that is able to define protein-binding affinities and identify physiochemical properties involved in protein binding for large numbers of PFAS. This proof-of-concept study was focused on the major serum transport protein albumin because of its critical role in PFAS distribution and bioaccumulation. However, because of the flexibility of this assay, PFAS binding properties of other purified proteins from any species of interest can be evaluated. Key parameters identified as determinants of PFAS HSA binding included the constitutive functional groups and the number of aliphatic carbons. Disruption of the aliphatic chain was found to decrease HSA-binding affinity and potentially alter the modes of binding. This was especially evident for the tetrafluoroethyl ether E1, which lacked a charged functional group but unlike fluorotelomer alcohols, was bound by HSA, a finding that suggests binding of this short-chain PFAS may be similar to HSA binding of volatile fluoroether anesthetics. Adaptation of the DSF methods demonstrated here will allow rapid

characterization of protein affinity for PFAS, improve computational modeling of protein-PFAS binding kinetics, and allow prioritization of PFAS for subsequent toxicity evaluation.

Funding

The research reported in this publication was supported by the National Institute of Environmental Health Sciences of the National Institutes of Health under Award Numbers P42ES031009 and T32ES007046. The content is solely the responsibility of the authors and does not necessarily represent the official views of the National Institutes of Health. Additional support was provided by an NC State University Office of Undergraduate Research Summer Fellowship.

REFERENCES

(1). Buck RC; Franklin J; Berger U; Conder JM; Cousins IT; de Voogt P; Jensen AA; Kannan K; Mabury SA; van Leeuwen SPJ Perfluoroalkyl and polyfluoroalkyl substances in the environment: terminology, classification, and origins. Integr. Environ. Assess. Manage 2011, 7, 513–541.

(2). Wang Z; Cousins IT; Scheringer M; Buck RC; Hungerbühler K Global emission inventories for C4-C14 perfluoroalkyl carboxylic acid (PFCA) homologues from 1951 to 2030, part II: the remaining pieces of the puzzle. Environ. Int 2014, 69, 166–176. [PubMed: 24861268]

(3). Prevedouros K; Cousins IT; Buck RC; Korzeniowski SH Sources, fate and transport of perfluorocarboxylates. Environ. Sci. Technol 2006, 40, 32–44. [PubMed: 16433330]

(4). Houde M; De Silva AO; Muir DCG; Letcher RJ Monitoring of perfluorinated compounds in aquatic biota: an updated review. Environ. Sci. Technol 2011, 45, 7962–7973. [PubMed: 21542574]

(5). Organisation for Economic Co-operation and Development. Toward a New Comprehensive Global Database of Per-and Polyfluoroalkyl Substances (PFASs): Summary Report on Updating the OECD 2007 List of per-and Polyfluoroalkyl Substances (PFASs), 2018.

(6). Fourth meeting of the Conference of the Parties to the Stockholm Convention on Persistent Organic Pollutants. Establishing indicative elements of a work programme to facilitate the elimination of listed brominated diphenyl ethers and the restriction or elimination of perfluorooctane sulfonic acid and its salts, perfluorooctane sulfonyl fluoride and other chemicals listed in Annexes A or B of the Convention at the fourth meeting of the Conference of the Parties, 2009.

(7). Bowman JS Fluorotechnology is critical to modern life: the FluoroCouncil counterpoint to the Madrid Statement. Environ. Health Perspect 2015, 123, A112–113. [PubMed: 25933200]

(8). Organization for Economic Co-operation and Development (OECD). Results of the 2006 OECD Survey on Production and Use of PFOS, PFAS, PFOA, PFCA, Their Related Substances and Products/Mixtures Containing These Substances, 2006.

(9). Guillette TC; McCord J; Guillette M; Polera ME; Rachels KT; Morgeson C; Kotlarz N; Knappe DRU; Reading BJ; Strynar M; Belcher SM Elevated levels of per- and polyfluoroalkyl substances in Cape Fear River Striped Bass (Morone saxatilis) are associated with biomarkers of altered immune and liver function. Environ. Int 2020, 136, No. 105358. [PubMed: 32044175]

(10). Kotlarz N; McCord J; Collier D; Lea CS; Strynar M; Lindstrom AB; Wilkie AA; Islam JY; Matney K; Tarte P; Polera ME; Burdette K; DeWitt J; May K; Smart RC; Knappe DRU; Hoppin JA Measurement of Novel, Drinking Water-Associated PFAS in Blood from Adults and Children in Wilmington, North Carolina. Environ. Health Perspect 2020, 128, No. 077005.

(11). Brusseau ML; Anderson RH; Guo B PFAS concentrations in soils: Background levels versus contaminated sites. Sci. Total Environ 2020, 740, No. 140017. [PubMed: 32927568]

(12). Cheng W; Ng CA A Permeability-Limited Physiologically Based Pharmacokinetic (PBPK) Model for Perfluorooctanoic acid (PFOA) in Male Rats. Environ. Sci. Technol 2017, 51, 9930–9939. [PubMed: 28759222]

(13). Cheng W; Ng CA Predicting Relative Protein Affinity of Novel Per- and Polyfluoroalkyl Substances (PFASs) by An Efficient Molecular Dynamics Approach. Environ. Sci. Technol 2018, 52, 7972–7980. [PubMed: 29897239]

(14). Forsthuber M; Kaiser AM; Granitzer S; Hassl I; Hengstschläger M; Stangl H; Gundacker C Albumin is the major carrier protein for PFOS, PFOA, PFHxS, PFNA and PFDA in human plasma. Environ. Int 2020, 137, No. 105324. [PubMed: 32109724]

(15). Layton CJ; Hellinga HW Quantitation of protein-protein interactions by thermal stability shift analysis. Protein Sci. 2011, 20, 1439–1450. [PubMed: 21674662]

(16). Vedadi M; Niesen FH; Allali-Hassani A; Fedorov OY; Finerty PJ; Wasney GA; Yeung R; Arrowsmith C; Ball LJ; Berglund H; Hui R; Marsden BD; Nordlund P; Sundstrom M; Weigelt J; Edwards AM Chemical screening methods to identify ligands that promote protein stability, protein crystallization, and structure determination. Proc. Natl. Acad. Sci. U.S.A 2006, 103, 15835–15840. [PubMed: 17035505]

(17). Niesen FH; Berglund H; Vedadi M The use of differential scanning fluorimetry to detect ligand interactions that promote protein stability. Nat. Protoc 2007, 2, 2212–2221. [PubMed: 17853878]

(18). Senisterra G; Chau I; Vedadi M Thermal denaturation assays in chemical biology. Assay Drug Dev. Technol 2012, 10, 128–136. [PubMed: 22066913]

(19). Simeonov A Recent developments in the use of differential scanning fluorometry in protein and small molecule discovery and characterization. Expert Opin. Drug Discovery 2013, 8, 1071–1082.

(20). Matulis D; Kranz JK; Salemme FR; Todd MJ Thermodynamic stability of carbonic anhydrase: measurements of binding affinity and stoichiometry using ThermoFluor. Biochemistry 2005, 44, 5258–5266. [PubMed: 15794662]

(21). Senisterra GA; Markin E; Yamazaki K; Hui R; Vedadi M; Awrey DE Screening for ligands using a generic and high-throughput light-scattering-based assay. J. Biomol. Screening 2006, 11, 940–948.

(22). Liberatore HK; Jackson SR; Strynar MJ; McCord JP Solvent Suitability for HFPO-DA ("GenX" Parent Acid) in Toxicological Studies. Environ. Sci. Technol. Lett 2020, 7, 477–481. [PubMed: 32944590]

(23). Savitzky A; Golay MJE Smoothing and Differentiation of Data by Simplified Least Squares Procedures. Anal. Chem 1964, 36, 1627–1639.

(24). Vivoli M; Novak HR; Littlechild JA; Harmer NJ Determination of Protein-ligand Interactions Using Differential Scanning Fluorimetry. J. Visualized Exp 2014, No. 51809.

(25). Ràfols C; Amézqueta S; Fuguet E; Bosch E Molecular interactions between warfarin and human (HSA) or bovine (BSA) serum albumin evaluated by isothermal titration calorimetry (ITC), fluorescence spectrometry (FS) and frontal analysis capillary electrophoresis (FA/CE). J. Pharm. Biomed. Anal 2018, 150, 452–459. [PubMed: 29291587]

(26). Hebert PC; MacManus-Spencer LA Development of a fluorescence model for the binding of medium- to long-chain perfluoroalkyl acids to human serum albumin through a mechanistic evaluation of spectroscopic evidence. Anal. Chem 2010, 82, 6463–6471. [PubMed: 20590160]

(27). Chen Y-M; Guo L-H Fluorescence study on site-specific binding of perfluoroalkyl acids to human serum albumin. Arch. Toxicol 2009, 83, 255–261. [PubMed: 18854981]

(28). Sabín J; Prieto G; González-Pérez A; Ruso JM; Sarmiento F Effects of fluorinated and hydrogenated surfactants on human serum albumin at different pHs. Biomacromolecules 2006, 7, 176–182. [PubMed: 16398513]

(29). Han X; Snow TA; Kemper RA; Jepson GW Binding of perfluorooctanoic acid to rat and human plasma proteins. Chem. Res. Toxicol 2003, 16, 775–781. [PubMed: 12807361]

(30). Bischel HN; Macmanus-Spencer LA; Luthy RG Noncovalent interactions of long-chain perfluoroalkyl acids with serum albumin. Environ. Sci. Technol 2010, 44, 5263–5269. [PubMed: 20540534]

(31). Beesoon S; Martin JW Isomer-Specific Binding Affinity of Perfluorooctanesulfonate (PFOS) and Perfluorooctanoate (PFOA) to Serum Proteins. Environ. Sci. Technol 2015, 49, 5722–5731. [PubMed: 25826685]

(32). Takehara K; Yuki K; Shirasawa M; Yamasaki S; Yamada S Binding properties of hydrophobic molecules to human serum albumin studied by fluorescence titration. Anal. Sci 2009, 25, 115–120. [PubMed: 19139584]

(33). Spector AA Fatty acid binding to plasma albumin. J. Lipid Res 1975, 16, 165–179. [PubMed: 236351]

(34). Lee IY; McMenamy RH Location of the medium chain fatty acid site on human serum albumin. Residues involved and relationship to the indole site. J. Biol. Chem 1980, 255, 6121–6127. [PubMed: 7391008]

(35). Ràfols C; Zarza S; Bosch E Molecular interactions between some non-steroidal anti-inflammatory drugs (NSAID's) and bovine (BSA) or human (HSA) serum albumin estimated by means of isothermal titration calorimetry (ITC) and frontal analysis capillary electrophoresis (FA/CE). Talanta 2014, 130, 241–250. [PubMed: 25159405]

(36). Wu L-L; Gao H-W; Gao N-Y; Chen F-F; Chen L Interaction of perfluorooctanoic acid with human serum albumin. BMC Struct. Biol 2009, 9, No. 31. [PubMed: 19442292]

(37). Vorum H; Pedersen AO; Honoré B Fatty acid and drug binding to a low-affinity component of human serum albumin, purified by affinity chromatography. Int. J. Pept. Protein Res 1992, 40, 415–422. [PubMed: 1483836]

(38). Honoré B; Brodersen R Detection of carrier heterogeneity by rate of ligand dialysis: medium-chain fatty acid interaction with human serum albumin and competition with chloride. Anal. Biochem 1988, 171, 55–66. [PubMed: 3407921]

(39). Curry S Plasma Albumin as a Fatty Acid Carrier. In Advances in Molecular and Cell Biology; Elsevier, 2003; Vol. 33, pp 29–46.

(40). Salvalaglio M; Muscionico I; Cavallotti C Determination of energies and sites of binding of PFOA and PFOS to human serum albumin. J. Phys. Chem. B 2010, 114, 14860–14874. [PubMed: 21028884]

(41). Dalvi VH; Rossky PJ Molecular origins of fluorocarbon hydrophobicity. Proc. Natl. Acad. Sci. U.S.A 2010, 107, 13603–13607. [PubMed: 20643968]

(42). Ng CA; Hungerbuehler K Exploring the Use of Molecular Docking to Identify Bioaccumulative Perfluorinated Alkyl Acids (PFAAs). Environ. Sci. Technol 2015, 49, 12306–12314. [PubMed: 26393377]

(43). Liu R; Eckenhoff RG Weak polar interactions confer albumin binding site selectivity for haloether anesthetics. Anesthesiology 2005, 102, 799–805. [PubMed: 15791110]

(44). Lo M-C; Aulabaugh A; Jin G; Cowling R; Bard J; Malamas M; Ellestad G Evaluation of fluorescence-based thermal shift assays for hit identification in drug discovery. Anal. Biochem 2004, 332, 153–159. [PubMed: 15301960]

(45). Ericsson UB; Hallberg BM; Detitta GT; Dekker N; Nordlund P Thermofluor-based high-throughput stability optimization of proteins for structural studies. Anal. Biochem 2006, 357, 289–298. [PubMed: 16962548]

(46). Epps DE; Sarver RW; Rogers JM; Herberg JT; Tomich PK The ligand affinity of proteins measured by isothermal denaturation kinetics. Anal. Biochem 2001, 292, 40–50. [PubMed: 11319816]

(47). Gao K; Oerlemans R; Groves MR Theory and applications of differential scanning fluorimetry in early-stage drug discovery. Biophys. Rev 2020, 12, 85–104. [PubMed: 32006251]

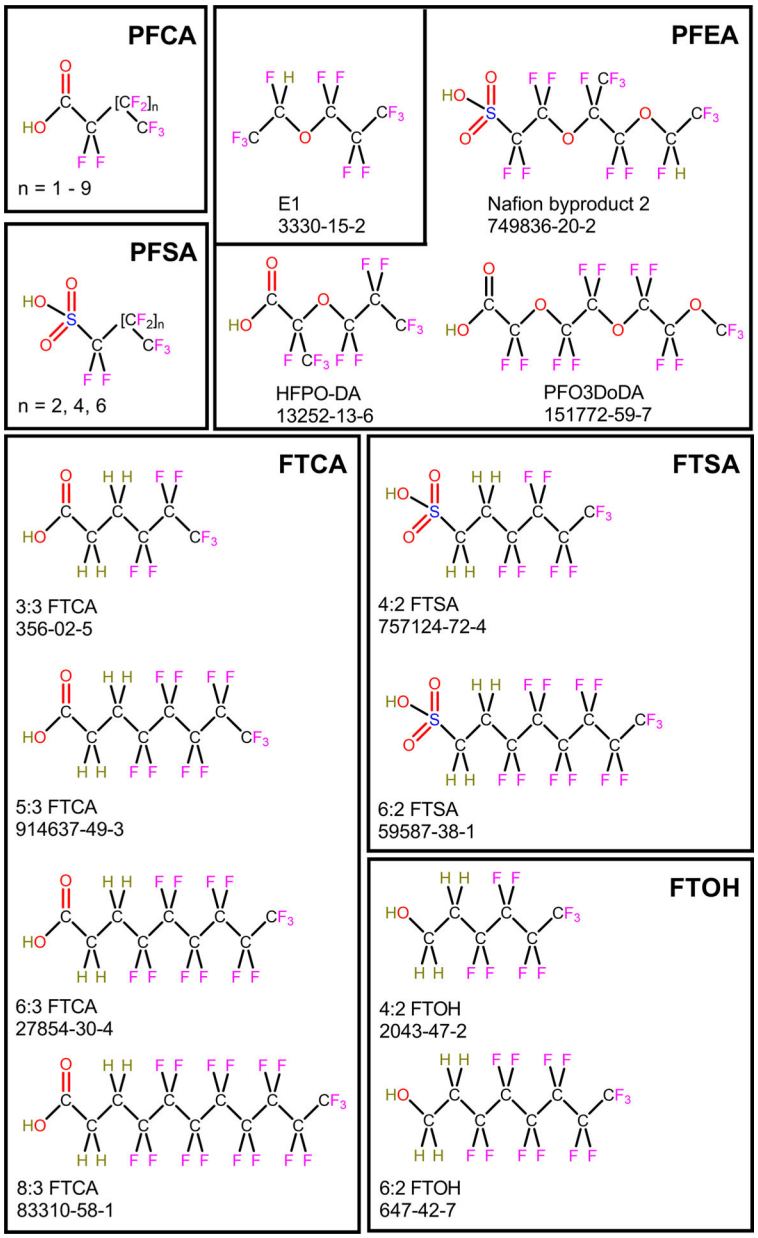

Figure 1.
Structures of PFAS analyzed.

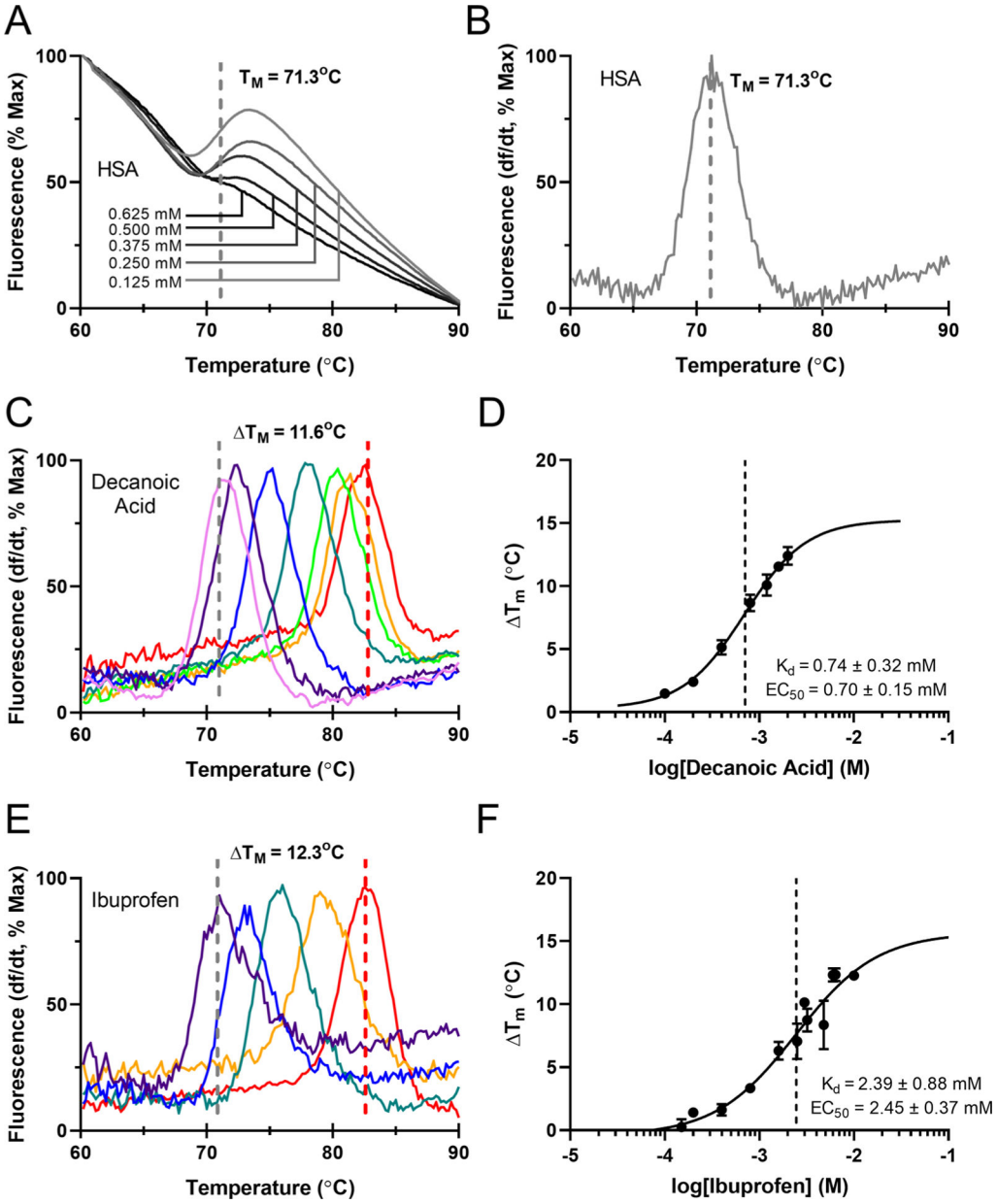

Figure 2.

Validation of DSF for measuring control compound binding. The fluorescence of HSA alone, normalized to the percentage maximum, as the temperature was increased from 60 to 90 °C is shown with the melting temperature indicated as the point at which half of the protein is inferred to be unfolded (A). Increasing concentrations of HSA (0.125–0.625 mM) from light gray to black are shown. The fluorescence signal of concentrations below 0.125 mM was not detectable. The derivative fluorescence of HSA alone, plotted as the derivative of fluorescence divided by the derivative of time, as the temperature was increased from 60 to 90 °C is shown with the melting temperature indicated as the maximum of the derivative curve (B). Derivative fluorescent curves for HSA with the fatty acid decanoic acid (C) or known albumin-binding compound ibuprofen (E) as the temperature was increased

from 60 to 90 °C, are shown with increasing concentrations of compounds indicated by increasing wavelength of color from violet to red. The maximum change in temperature for HSA alone is shown between the dashed gray and red lines. The regression of the change in temperature plotted against the logarithmic transformed concentration, in molar units is shown for decanoic acid (D) and ibuprofen (F), with the log(EC_{50}) indicated by a dashed line. $n \geq 3$ across at least two replicate plates for all compounds.

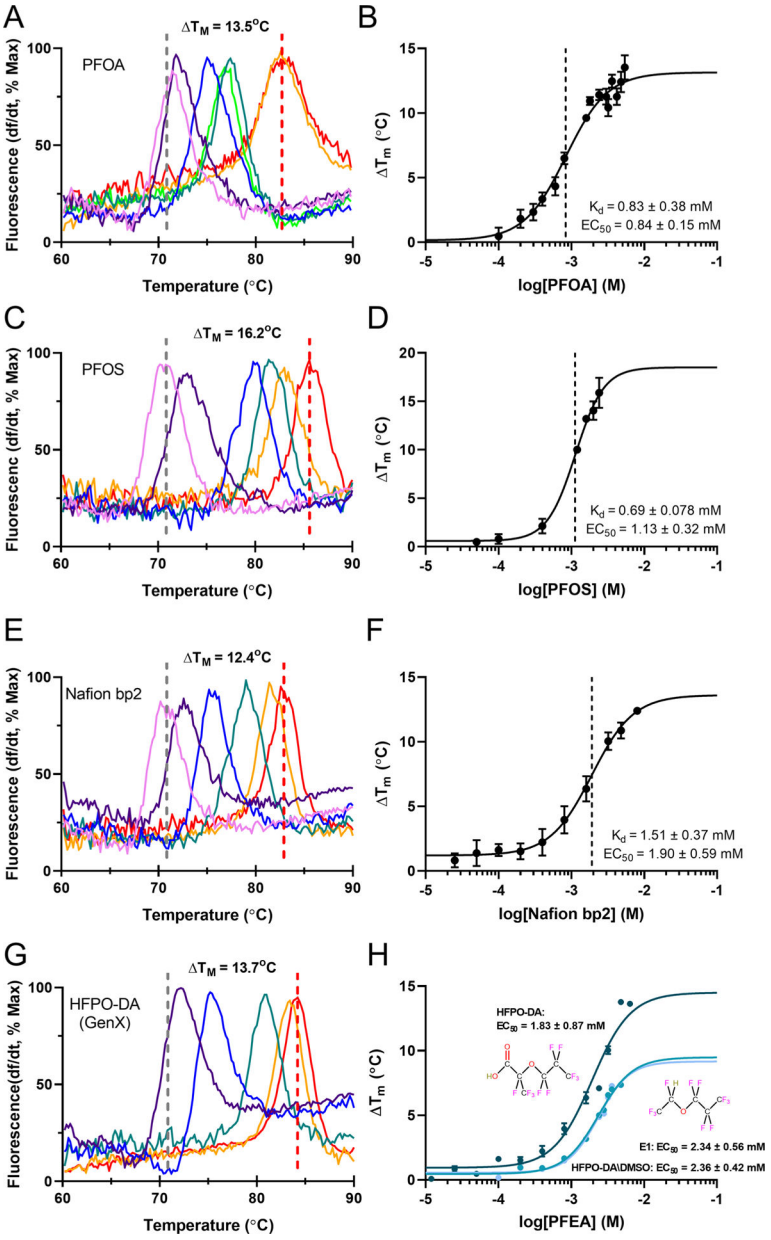

Figure 3.

Validation of DSF for measuring PFAS binding. Derivative fluorescent curves for HSA with the PFAA PFOA (A), PFOS (C), Nafion byproduct 2 (E), and HFPO-DA (GenX) (G), as the temperature was increased from 60 to 90 °C, are shown with increasing concentrations of the compound indicated by increasing wavelength of color from violet to red. The maximum change in temperature from HSA alone is shown between the dashed gray and red lines. The regression of the change in temperature plotted against the logarithmic transformed concentration, in molar units, is shown for PFOA (B), PFOS (D), Nafion byproduct 2 (F), and GenX (H) with the log(EC_{50}) indicated by a dashed line. $n \geq 3$ across at least two replicate plates for all compounds. In panel (H), the regression of the change in temperature

plotted against the logarithmic transformed concentration, in molar units, is also shown for GenX in DMSO and E1, along with chemical structures for GenX and E1.

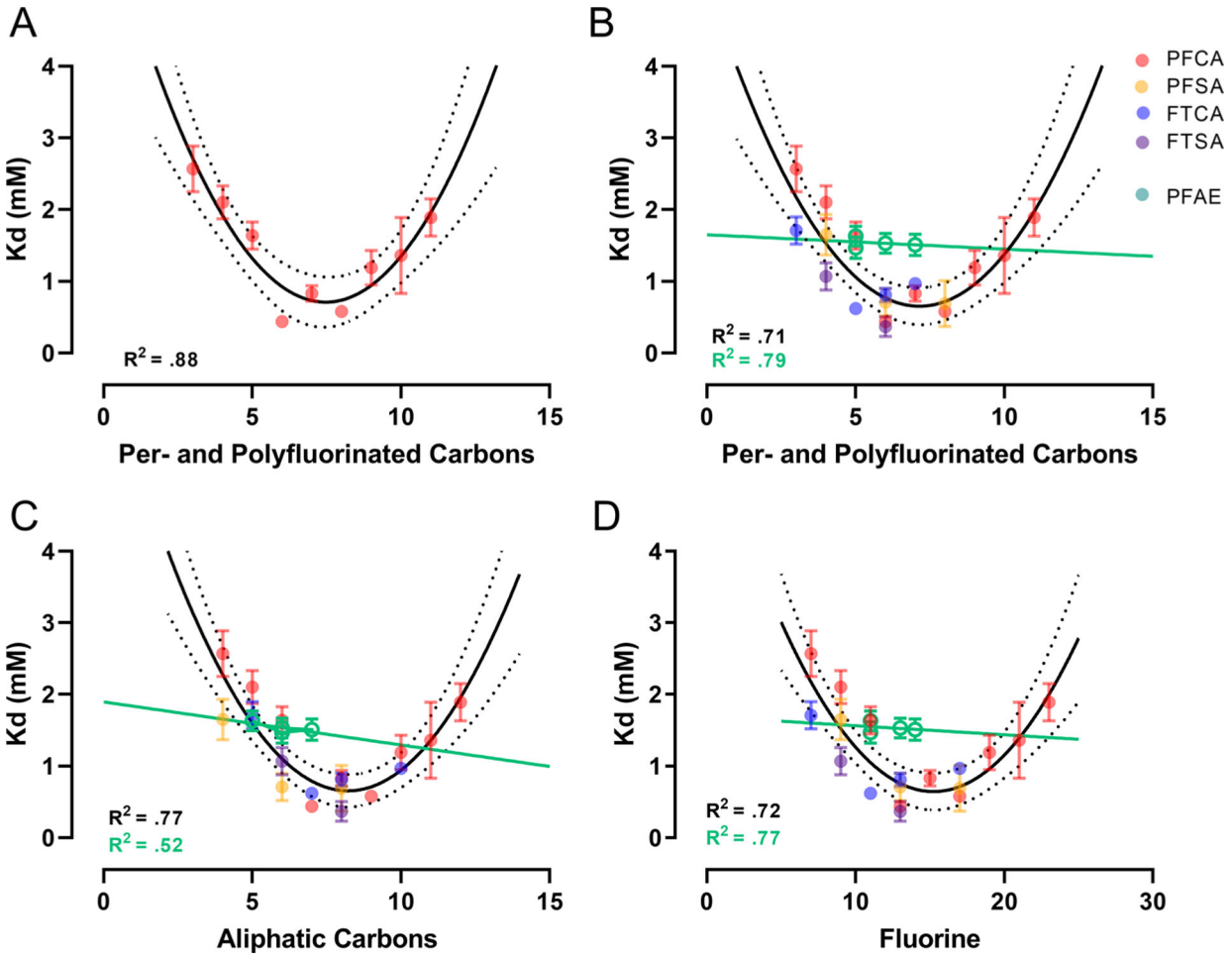

Figure 4.

Effect of carbon chain length and fluorine moieties on PFAS binding. The binding affinities of PFCA (A) and all analyzed PFAA and PFAE (B–D) are plotted against the number of per- and polyfluorinated carbons (A, B), aliphatic carbons, (C), or fluorine (D). For all PFAA except PFAE, a quadratic line of best fit with 95% confidence interval in dashed lines was generated using least-squares regression. Each class is indicated by different colors, with PFCA in red, PFSA in orange, PFAE in green, FTCA in blue, and FTSA in purple. $n \geq 3$ across at least two replicate plates for all compounds.

Table 1.

Analysis of Solvent Effects

solvent	K_d (mM)	EC_{50} (mM)	ΔT_m (°C)
HEPES-buffered saline (HBS)	0.83 ± 0.27	0.84 ± 0.10	13.5 ± 0.26
methanol (30% in HBS)	0.83 ± 0.15	0.78 ± 0.17	13.5 ± 0.19
DMSO (5 M in HBS)	0.84 ± 0.20	0.85 ± 0.02	13.2 ± 0.35

[a] ΔT_m is in °C. EC_{50} and K_d are mean values reported in ± SD. Each compound was run on at least two separate plates with $n \geq 4$.

Table 2.

Binding Affinity of HSA for Control Compounds[a]

compounds	CAS ID	R^2	ΔT_m (°C)	EC_{50} (mM)	K_d (mM)
octanoic acid	124-07-2	0.93	3.1 ± 0.17	2.15 ± 0.25	2.10 ± 0.47
decanoic acid	334-48-5	0.98	12.4 ± 0.50	0.70 ± 0.15	0.74 ± 0.32
hexadecanoic acid	57-10-3	0.95	7.2 ± 0.13	0.084 ± 0.05	0.03 ± 0.02
ibuprofen	15687-27-1	0.97	12.3 ± 0.24	2.45 ± 0.37	2.39 ± 0.88
warfarin	81-81-2	0.97	9.3 ± 0.21	0.19 ± 0.06	0.16 ± 0.10

[a] ΔT_m is in °C, EC_{50} and K_d are mean values reported in ± SD. Each compound was run on at least two separate plates with $n \geq 4$.

Table 3.

Binding Affinity of HSA for PFAS[a]

PFAS	CAS ID	chain length	aliphatic carbons	fluorines	R^2	ΔT_m (°C)	EC_{50} (mM)	K_d (mM)
			PFCA					
PFBA	375-224	3	4	7	0.94	6.48 ± 0.18	2.61 ± 0.47	2.57 ± 0.78
PFPeA	2706-90-3	4	5	9	0.97	13.1 ± 0.066	2.14 ± 0.42	2.10 ± 0.56
PFHxA	307-244	5	6	11	0.98	10.6 ± 0.24	1.40 ± 0.27	1.64 ± 0.47
PFHpA	375-86-9	6	7	13	0.95	15.3 ± 0.41	0.68 ± 0.15	0.44 ± 0.20
PFOA	335-67-1	7	8	15	0.97	13.5 ± 0.41	0.84 ± 0.15	0.83 ± 0.38
PFNA	375-95-1	8	9	17	0.97	13.4 ± 0.34	0.60 ± 0.23	0.58 ± 0.21
PFDA	335-76-2	9	10	19	0.99	17.2 ± 0.13	1.11 ± 0.17	1.19 ± 0.59
PFunDA	2058-94-8	10	11	21	0.98	9.02 ± 0.47	1.49 ± 0.048	1.36 ± 1.06
PFDoA	307-55-1	11	12	23	0.98	7.74 ± 0.20	2.51 ± 0.34	1.89 ± 0.64
			PFSA					
PFBS	375-73-5	4	4	9	0.96	11.9 ± 0.11	1.72 ± 0.56	1.65 ± 0.69
PFHxS	3871-99-6	6	6	13	0.98	11.0 ± 0.24	0.98 ± 0.069	0.71 ± 0.47
PFOS	2795-39-3	8	8	17	0.98	16.2 ± 0.90	1.13 ± 0.32	0.69 ± 0.078
			Per- and Polyfluorinated Alkyl Ethers					
E1	3330-15-2	5	5	11	0.93	7.32 ± 0.059	2.34 ± 0.56	1.64 ± 0.34
HFPO-DA	13252-13-6	5	5	11	0.97	13.7 ± 0.17	1.83 ± 0.87	1.60 ± 0.55
Nafion bp2	749836-20-2	7	7	14	0.98	12.4 ± 0.17	1.90 ± 0.59	1.51 ± 0.37
PFO3DoDA	151772-59-7	6	7	13	0.95	20.6 ± 0.82	1.67 ± 0.47	1.53 ± 0.34
			Fluorotelomer Alcohols					
4:2 FTOH	204 3 47-2	4	6	9	N/A	0 ± 0	N/A	N/A
6:2 FTOH	64742-7	6	8	13	N/A	0 ± 0	N/A	N/A
			Fluorotelomer Carboxylic Acids					
3:3 FTCA	356-02-5	3	6	7	0.81	2.24 ± 0.062	2.06 ± 0.51	1.71 ± 0.47
5:3 FTCA	91463749-3	6	8	11	0.94	3.62 ± 0.14	1.48 ± 0.24	0.62 ± 0.10
6:3 FTCA	27854-304	6	9	13	0.95	9.50 ± 0.20	0.84 ± 0.21	0.81 ± 0.23
8:3 FTCA	83310-584	8	11	17	0.89	10.01 ± 0.17	1.16 ±0.42	0.97 ±0.17
			Fluorotelomer Sulfonic Acids					

PFAS	CAS ID	chain length	aliphatic carbons	fluorines	R^2	ΔT_m (°C)	EC_{50} (mM)	K_d (mM)
4:2 FTSA	757124-724	4	6	9	0.93	3.49 ± 0.12	1.45 ± 0.34	1.07 ± 0.47
6:2 FTSA	59587-38-1	6	8	13	0.91	3.60 ± 0.47	0.47 ± 0.29	0.37 ± 0.34

[a]Chain length is the number of per/polyfluorinated carbons; ΔT_m is in °C, EC_{50} and K_d are mean values reported in + SD. Each compound was run on at least two separate plates with $n \geq 4$.